Volume 281, number 1,2, 240–244 FEBS 09597 April 1991

ADONIS 001457939100306F

Contribution of proline-14 to the structure and actions of melittin

Christopher E. Dempsey[1], Renzo Bazzo[1], Timothy S. Harvey[1], Inge Syperek[2], Gunther Boheim[2] and Iain D. Campbell[1]

[1] *Biochemistry Department, Oxford University, South Parks Road, Oxford OX1 3QU, UK* and [2] *Department of Zellphysiologie, Ruhr Universitat Bochum, Postfach 102148, D-4630 Bochum 1, Germany*

Received 18 January 1991

The structure and dynamic properties of bee venom melittin and a synthetic analogue, [Ala[14]]-melittin (melittin P14A), are compared, using high resolution ^{1}H nuclear magnetic resonance (NMR) spectroscopy and amide exchange measurements in methanol. P14A is shown to adopt a regular, stable α-helical conformation in solution without the flexibility around the Pro-14 residue found in melittin. P14A has twice the hemolytic activity of melittin but is less able to induce voltage-dependent ion conductance in planar bilayers. The results indicate that helix flexibility afforded by the Pro-14 residue promotes the ability of melittin to adopt the transbilayer associates thought to underlie ion translocation.

Melittin; [Ala[14]]-Melittin; Nuclear magnetic resonance, ^{1}H; Hydrogen exchange; Hemolysis; Membrane channel

1. INTRODUCTION

Proline residues commonly occur within the putative membrane-spanning α-helices of membrane transport and receptor proteins and within the amphipathic helices of channel-forming peptides like alamethicin and melittin [1,2]. Several roles for proline have been proposed to explain its high occurrence in these structures including the ability of the X-Pro bond to undergo *cis–trans* isomerism [3], the exposure of a backbone peptide carbonyl as a coordination [4] or proton binding site [5] or the introduction of a bend in the helix [6,7].

Melittin, a 26 amino acid peptide from bee venom that lyses cell membranes and induces voltage-dependent ion conductance in planar lipid bilayers [8–11], contains a proline at residue 14 near the centre of the sequence. The conformation of melittin is relatively well understood in a variety of solvents; it adopts an α-helical conformation in water at high concentrations [12], in methanol [13] and when bound to micelles [14]. There is considerable flexibility around the P14 residue as demonstrated, for example, by hydrogen exchange measurements [15,16]. To determine the contribution of proline to the structural and functional properties of melittin we are studying the properties of a synthetic analogue with a Pro-14 → Ala substitution (melittin P14A) [17]. Here we compare the structural and dynamic properties of melittin and P14A in solution using high resolution ^{1}H nuclear magnetic resonance (NMR) spectroscopy and amide exchange measurements and illustrate the effects of the Pro → Ala substitution on the membrane actions of melittin (hemolysis and voltage-dependent ion conductance).

Correspondence address: C.E. Dempsey, Biochemistry Department, Bristol University, School of Medical Sciences, Bristol BS8 1TD, UK

2. MATERIALS AND METHODS

2.1. *Peptides*

Synthetic P14A, and melittin from bee venom, were purified as described [17]. Rechromatography of melittin on a Vydac C4 reverse phase column [17] resulted in peptide free of detectable phospholipase activity.

2.2. *^{1}H NMR and structural analysis*

NMR experiments were run on Bruker AM 500 and 600 spectrometers and the assignment of the ^{1}H NMR spectrum of the peptide backbone amides of P14A (Fig. 1) was done using two-dimensional NMR methods as described for melittin [13]. NOEs (Fig. 2A) were determined from a 2D NOESY experiment at 600 MHz using a mixing time of 250 ms. Molecular dynamics simulations, incorporating the NOE-derived distance constraints, were done as described in [16] from which the data for melittin was obtained. Amide hydrogen exchange measurements were made by following the time-dependence of the loss of amide intensity in the ^{1}H NMR spectrum after dissolving the peptide in CD_3OD [15] and the exchange data converted to hydrogen bond lifetimes [16].

2.3. *Hemolysis and planar bilayer conductance measurements*

Hemolysis assays were performed by following the release of hemoglobin from washed, recently outdated, human erythrocytes after adding peptide to a suspension of the cells. Aliquots of the suspension were removed over a time course, the cells rapidly pelleted in a microfuge (15 s) and the hemoglobin content of the supernatant determined from the absorbance at 578 nm [18].

For measurement of peptide-induced, voltage-dependent membrane conductance, planar lipid bilayers were formed from 1-palmitoyl, 2-oleoyl-phosphatidylcholine: dioleoyl-phosphatidylserine: cholesterol (75:25:5, M:M:M) in hexane using the Montal-Mueller method [19]. The aqueous compartments consisted of 4M NaCl and 10 mM Tris-HCl, pH 7.0. Other details are described in the legend to Fig. 4.

Published by Elsevier Science Publishers B.V.

Table I

Comparison of $^3J_{NHC^{\alpha}H}$ coupling constants for melittin and P14A

Residue	$^3J_{NHC^{\alpha}H}$	
	melittin	P14A
1	-	-
2	4.1	4.0
3	5.2/5.8	4.8/5.8
4	4.3	4.2
5	5.5	5.1
6	4.0	4.4
7	4.4	4.6*
8	5.1	-
9	4.8	4.2*
10	6.6	4.4*
11	7.3	4.6**
12	5.5/5.5	5.1/6.0
13	3.7	4.6
14	-	4.1
15	5.3	4.4
16	5.0	4.4
17	4.6	4.6
18	2.9*	3.4
19	4.5	4.6
20	4.4	4.6
21	4.1	4.4
22	4.7*	4.5
23	4.7	4.6*
24	4.8*	-
25	6.1	6.4
26	7.4	7.3

Coupling constants were measured from one-dimensional ^{1}H NMR spectra, in some cases under conditions of partial amide exchange to aid resolution of overlapping amide signals. Values marked with an asterisk are less precise because of poor spectral resolution or ambiguity over the assignment of the signal. The value for T11 of P14A was measured from a 2D NOESY spectrum. The digital resolution was 0.15 Hz/pt for melittin and 0.3 Hz/pt for P14A.

3. RESULTS AND DISCUSSION

We have previously studied the conformation and dynamics of melittin in methanol [13,15,16]. Using the same two-dimensional NMR procedures we have assigned the ^{1}H NMR spectrum of P14A. Analysis of the spectrum reveals that P14A adopts a relatively stable helical conformation between residues 3–24. This result is apparent from the small values (3–5 Hz) for $^3J_{NHC\alpha H}$ coupling constants [20] (Table I) and the slowly exchanging backbone amide hydrogens which correspond to the hydrogen-bonded amides expected in an α-helix. Compared with the corresponding amides in melittin, many of the P14A amide hydrogens have large downfield chemical shifts implying that these amides are involved in shorter hydrogen bonds [21] (Fig. 1); particularly large differences between melittin and P14A are observed for the chemical shifts of amides 10–15. Amides at the ends of the helices (residues 2–5 and 21–26) have very similar chemical shifts in both peptides.

We have analysed the NOEs observed for P14A shown in Fig. 2A. Using these data as restraints in molecular dynamics simulations [13,16], P14A is shown to form a more stable helix than melittin, especially in the central region (Fig. 2B).

Our previous studies have shown that monomeric melittin possesses considerable backbone flexibility in the region of residues 10–15. This was indicated by the large values of $^3J_{NHC^{\alpha}H}$ for T10 and T11, and the lack of NOEs and destabilization of hydrogen bonds involving the amide hydrogens of G12, L13 and A15. A measure of backbone flexibility can be obtained from the kinetics of single amide hydrogen exchange with solvent deuterons [22]. Exchange of hydrogen-bonded amides occurs during backbone fluctuations in which hydrogen bonds are transiently broken. These fluctuations are generally characterized as an equilibrium between hydrogen-bonded ('closed') conformers and 'open' conformers [23]:

$$NH_c \underset{k_2}{\overset{k_1}{\rightleftharpoons}} NH_o \xrightarrow{k_3} ND$$

Under the conditions of amide exchange from melittin in methanol [15], the fluctuation is in pre-equilibrium with chemical exchange ($k_2 \gg k_3$), and the measured exchange rate constant, k_{ex}, is equal to $K_0 k_3$, where K_0 ($= k_1/k_2$) characterises the hydrogen-bond-breaking conformational fluctuation. Within this model, the percentage occupancy of hydrogen bonds involving backbone amide hydrogens can be shown [16] to be $100/(1 + K_0)$%. A comparison of hydrogen bond occupancies for melittin and P14A amides is shown in Fig. 3. In melittin, the P14 residue destabilises the central turn of helix so that the N-terminal (G1-T11) and C-terminal (L13-Q26) helical segments are connected by a flexible 'hinge' [15,16]. Replacement of the central proline residue with alanine in P14A leads to a protection of amides in the central turn of helix by up to 40-fold indicating a large suppression of backbone fluctuations in this region of the helix. The effects are not localized to the centre of the helix but are transmitted throughout the molecule so that amides in the N- and C-terminal helical sections are stabilized to exchange by about 5–8-fold throughout. There is a general correlation between the extent of amide stabilization (Fig. 3) and the effect on the amide chemical shift (Fig. 1).

When washed human erythrocytes are incubated with micromolar concentrations of melittin, a biphasic release of hemoglobin is observed. The molecular events giving rise to the two kinetic phases are proposed to be due to initial disruptive binding of melittin to the outer leaflet of the bilayer followed by peptide internalization [24]. Melittin and P14A-induced hemolysis show similar biphasic kinetics but P14A is more effective (Fig. 4A); comparable release of hemoglobin occurs at half the concentration of P14A compared with

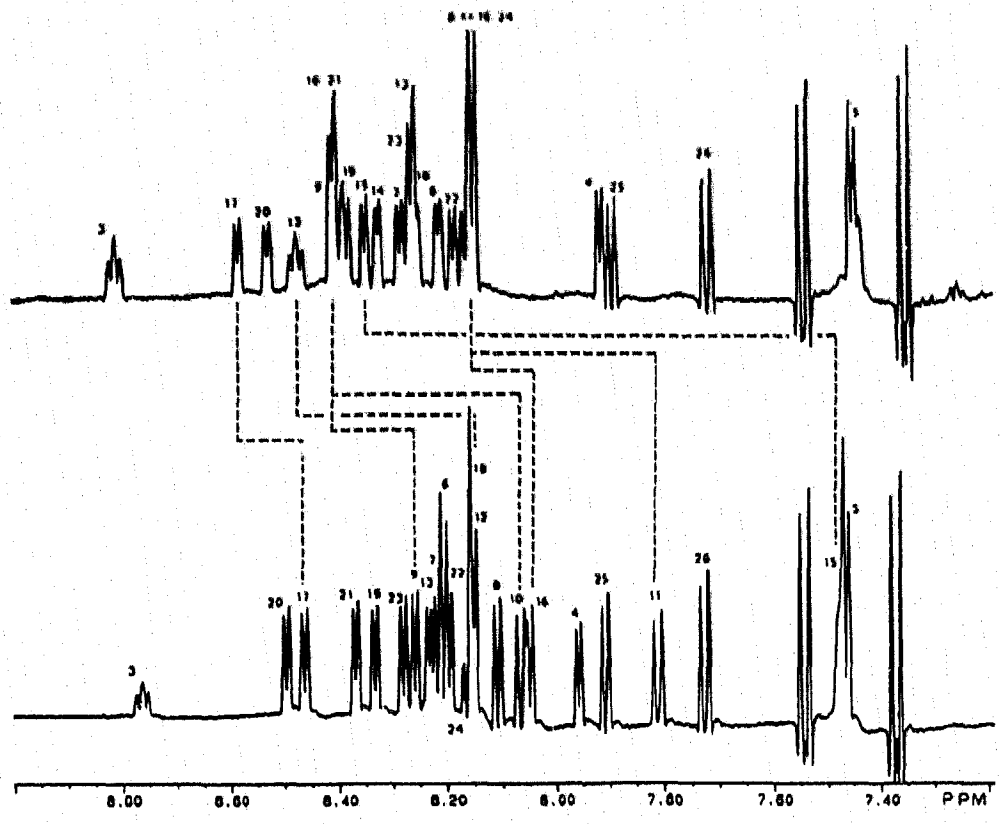

Fig. 1. Downfield region of the 500 MHz ^{1}H NMR spectra of melittin (bottom) and P14A (top) in methanol (CD_3OH). The amide NH resonances are numbered according to the peptide amino acid sequence. Unlabeled resonances belong to W19 indole ring protons.

melittin and similar results were obtained under a variety of peptide concentrations and ionic strengths (not shown). P14A was tested for its ability to induce voltage-dependent channel activity in planar lipid membranes [10], and was found to induce bilayer disruption except at high ionic strength (4 M NaCl) where the current/voltage relationship and current fluctuation data of Fig. 4B were recorded. At lower ionic strength ($\leq$1 M NaCl) application of a membrane potential to P14A-containing bilayers resulted in breakdown of the permeability barrier. The structure of the melittin channel formed under the influence of a transbilayer potential is proposed to share features of the alamethicin channel in which bent helical monomers in a transbilayer orientation are arranged in a cylindrical array around the channel axis [6]. According to this model, a bend in the centre of the helix induced by proline allows the charged C-terminal helical segments (containing the sequence Lys-Arg-Lys-Arg) to bend away from the channel axis minimising charge repulsion. In cylindrical arrays of the straight P14A helix, C-terminal electrostatic repulsion would destabilize the channel except at high ionic strength.

In multi-channel (I/V) measurements melittin is significantly more active under comparable conditions than P14A. A reference conductivity reached at 100 mV

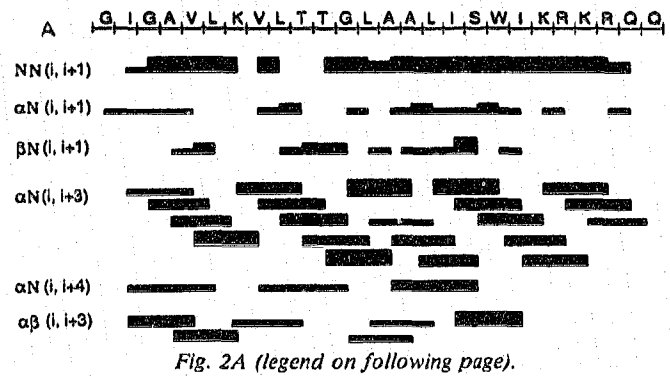

Fig. 2A (legend on following page).

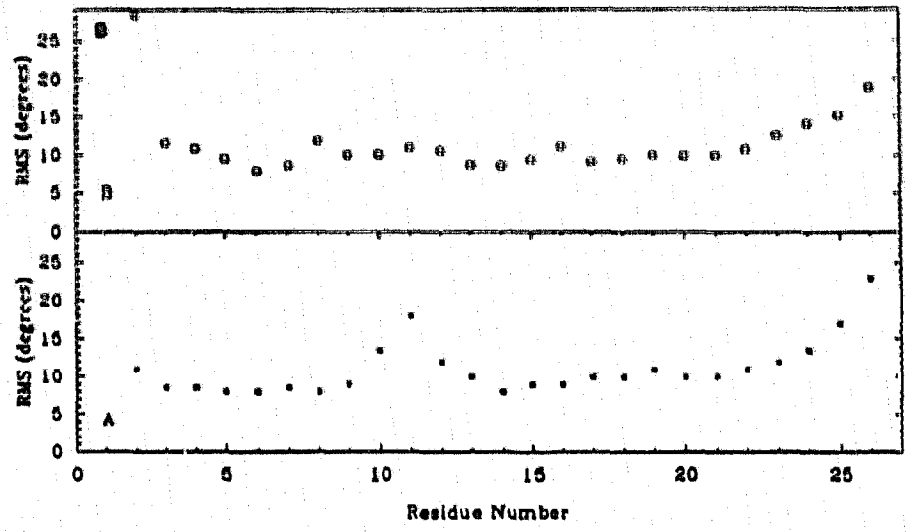

Fig. 2. (A) The NOEs observed for P14A in methanol classified according to their intensities (weak, medium, strong). Resonance overlap precluded the quantitation of some NOEs although the overlapped cross-peaks were consistent with the conclusions about conformation presented here; only unambiguous results are shown in the figure. (B) Plots of the root mean square deviation (rmsd) of phi for (A) melittin and (B) P14A during molecular dynamics simulations. The data for melittin were taken from Pastore *et al.* [16] and the simulations for P14A were done using the same protocol. Fewer distance restraints were obtained for P14A (97) than for melittin (193) mainly because of resonance overlap. This leads to somewhat higher rmsd values for P14A in some regions (e.g. in the N-terminal region).

in 1 M NaCl with melittin (Fig. 2b of ref. 10) requires a potential of 300 mV for P14A in 4 M NaCl (Fig. 4B), indicating a higher activation barrier for membrane insertion of P14A relative to melittin. The dissociation of hemolytic activity (enhanced) and voltage-dependent channel formation (suppressed) by substituting Pro-14 in melittin with Ala indicates that melittin-induced hemolysis is not a direct consequence of the formation of voltage-dependent channels. The high activity of P14A is consistent with models in which hemolysis results from the disruption of bilayer structure by an amphipathic helix [24,25] perhaps involving reorientation of the peptide under the influence of a transmembrane potential.

The results presented here demonstrate that the presence of proline considerably enhances backbone flexibility in the melittin α-helix and allows it to form more stable ion channels. We have found no evidence that proline exists in a *cis* conformation in melittin [13]. We believe that the increased flexibility arises because proline is unique among the common amino acids in its inability to form a backbone hydrogen bond (N_n–O_{n-4}). This missing hydrogen bond will break a single membrane-spanning helix and form a hinge which might facilitate the packing of helical bundles, the accommodation of receptor ligands or the structural changes accompanying proton pumping [26,27].

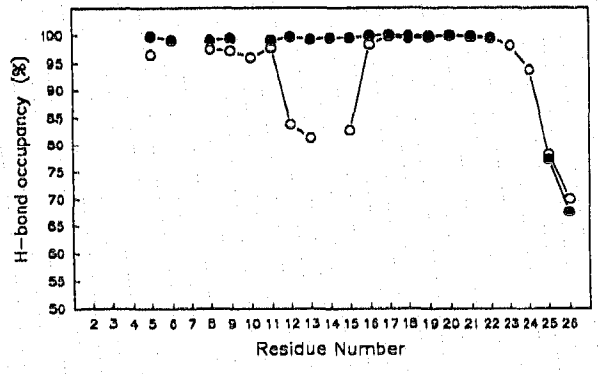

Fig. 3. Comparison of the hydrogen bond occupancy of individual amides in melittin (open circles) and P14A (closed circles) determined from pH-dependent amide exchange measurements [15]. Amides of residues 1–4 are not hydrogen-bonded and have 'zero' occupancy. Gaps in the sequence indicate either amides for which exchange could not be determined due to resonance overlap, or, for melittin, the absence of a P14 amide hydrogen. Individual exchange rates for V8 and T11 in P14A could not be resolved due to resonance overlap and the values for these amides are averages.

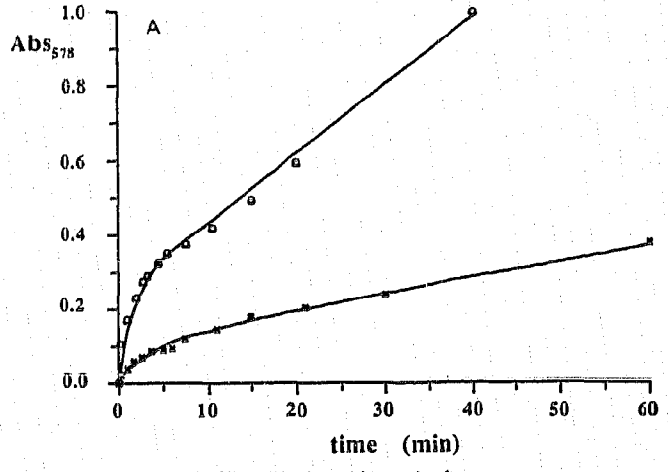

Fig. 4A (legend overleaf).

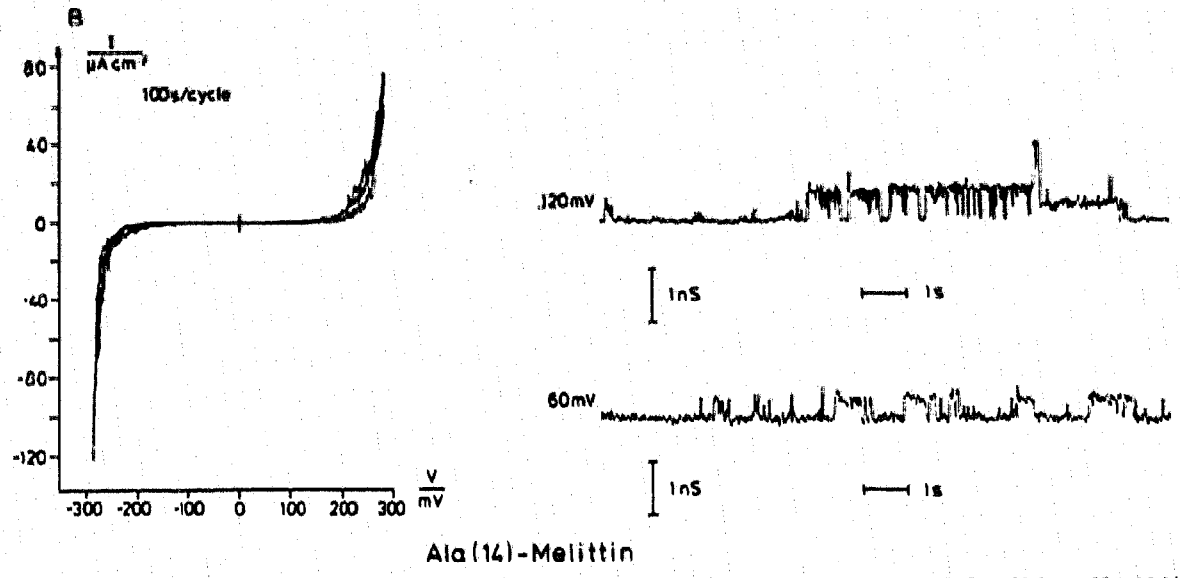

Fig. 4. (A) Time-dependence of the release of hemoglobin from washed human erythrocytes in 20 mM Tris-HCl, pH 7.4, 150 mM NaCl (37°C) containing 3.1×10^{-7} M melittin (×) or P14A (○). (B) Current/voltage relationship (left) and single channel recordings (right) for planar lipid bilayers containing P14A. For the *I/V* measurement at 26°C (left) P14A was added to both aqueous compartments at a concentration of $4\,\mu g \cdot ml^{-1}$ (1.2×10^{-6} M). For the single channel recordings, P14A was added only to the *cis* compartment at a concentration of $2\,\mu g \cdot ml^{-1}$. The upper recording (120 mV) was made at 26°C and the lower recording (60 mV) at 7°C.

Acknowledgements: This research was supported by grants from the Central Fund of Oxford University (to C.E.D.) and is a contribution from the Oxford Centre for Molecular Sciences which is supported by the SERC and MCR. We also thank the Wellcome Foundation for financial support and Charles Courquin for carrying out a number of early simulations on melittin and P14A.

REFERENCES

[1] Jennings, M.L. (1989) Annu. Rev. Biochem. 58, 223-256.
[2] Rees, D.C., Komiya, H., Yeates, T.O., Allen, J.P. and Feher, G. (1989) Annu. Rev. Biochem. 58, 607-633.
[3] Brandl, C.J. and Deber, C.M. (1986) Proc. Natl. Acad. Sci. USA 83, 917-921.
[4] Eisenman, G. and Dani, J.A. (1987) Annu. Rev. Biophys. Chem. 16, 205-226.
[5] Dunker, A.K. (1982) J. Theor. Biol. 97, 95-127.
[6] Fox, R.O. and Richards, F.M. (1982) Nature 300, 325-330.
[7] Barlow, D.J. & Thornton, J.M. (1988) J. Mol. Biol. 201, 601-619.
[8] Habermann, E. (1972) Science 177, 314-322.
[9] Tosteson, M.T. and Tosteson, D.C. (1981) Biophys. J. 36, 109-116.
[10] Hanke, W., Methfessel, C., Wilmsen, H.-U., Katz, E., Jung, J. and Boheim, G. (1983) Biochim. Biophys. Acta 727, 108-114.
[11] Dempsey, C.E. (1990) Biochim. Biophys. Acta 1032, 143-161.
[12] Terwilliger, T.C. and Eisenberg, D.J. (1982) Biol. Chem. 257, 6016-6022.
[13] Bazzo, R., Tappin, M.J., Pastore, A., Harvey, T.S., Carver, J.A. and Campbell, I.D. (1988) Eur. J. Biochem. 139-146.
[14] Inagaki, F., Shimada, I., Kawaguchi, K., Hirano, M., Terasawa, I., Ikura, T. and Gō, N. (1989) Biochemistry 18, 5985-5991.
[15] Dempsey, C.E. (1988) Biochemistry 27, 6893-6901.
[16] Pastore, A., Harvey, T.S., Dempsey, C.E. and Campbell, I.D. (1989) Eur. Biophys. J. 16, 363-367.
[17] Dempsey, C.E. and Sternberg, B. (1991) Biochim. Biophys. Acta (in press).
[18] Hider, R.C., Khader, F. and Tatham, A.S. (1983) Biochim. Biophys. Acta 728, 206-214.
[19] Montal, M. and Mueller, P. (1972) Proc. Natl. Acad. Sci. USA 69, 3561-3566.
[20] Wuthrich, K. (1986) NMR of Proteins and Nucleic Acids, Wiley, New York.
[21] Wagner, G., Pardi A. and Wuthrich, K. (1983) J. Am. Chem. Soc. 105, 5948-5949.
[22] Englander, S.W. and Kallenbach, N. (1984) Q. Rev. Biophys. 16, 521-655.
[23] Hvidt, A. and Nielsen, S.O. (1966) Adv. Prot. Chem. 21, 287-386.
[24] DeGrado, W.F., Musso, G.F., Lieber, M., Kaiser, E.T. and Kezdy, F. (1982) Biophys. J. 37, 329-338.
[25] Terwilliger, T.C., Weissman, L. and Eisenberg, D. (1982) Biophys. J. 37, 353-361.
[26] Gerwert, K., Hess, B. and Engelhard, M. (1990) FEBS Lett. 261, 449-454.
[27] Rothschild, K.J., He, Y.-W, Mogi, T., Marti, T., Stern, L.J. and Khorana, H.G. (1990) Biochemistry. 29, 5954-5960.